

EUROPEAN COMMISSION

HORIZON 2020 PROGRAMME
FUEL CELLS AND HYDROGEN JOINT UNDERTAKING (FCH 2 JU)
TOPIC H2020-JTI-FCH-2015-1
Improved electrolysis for distributed hydrogen production

GA No. 700008

High Performance PEM Electrolyser for Cost-effective Grid Balancing Applications



HPeM₂GAS - Deliverable report

D4.5 Publishable report on MEA development and characterisation

Deliverable No.	HPEM2GAS D4.1	
Related WP	4	
Deliverable Title	Publishable report on MEA development and characterisation	
Deliverable Date	2018-07-23	
Deliverable Type	REPORT	
Dissemination level	Public	
Author(s)	Laila Grahl-Madsen (EWII) Stefania Siracusano, Nicola Briguglio, Stefano Trocino, Vincenzo Baglio, Antonino Aricò (CNR-ITAE) Stefano Tonella, Claudio Oldani, Luca Merlo (Solvay) Daniel A. Greenhalgh and Ben Green (ITM-Power)	
Checked by	Laila Grahl-Madsen (EWII)	
Reviewed by (if applicable)	n/a	
Approved by	Antonino Aricò (CNR-ITAE) - Coordinator	23 July 2018
Status	Final	

Disclaimer/ Acknowledgment



Copyright ©, all rights reserved. This document or any part thereof may not be made public or disclosed, copied or otherwise reproduced or used in any form or by any means, without prior permission in writing from the HPEM2GAS Consortium. Neither the HPEM2GAS Consortium nor any of its members, their officers, employees or agents shall be liable or responsible, in negligence or otherwise, for any loss, damage or expense whatever sustained by any person as a result of the use, in any manner or form, of any knowledge, information or data contained in this document, or due to any inaccuracy, omission or error therein contained.

All Intellectual Property Rights, know-how and information provided by and/or arising from this document, such as designs, documentation, as well as preparatory material in that regard, is and shall remain the exclusive property of the HPEM2GAS Consortium and any of its members or its licensors. Nothing contained in this document shall give, or shall be construed as giving, any right, title, ownership, interest, license or any other right in or to any IP, know-how and information.

This project has received funding from the FCH JU and European Union's Horizon 2020 research and innovation programme under grant agreement No 700008. This Joint Undertaking receives support from the European Union's Horizon 2020 research and innovation programme and Hydrogen Europe and Hydrogen Europe Research

The information and views set out in this publication does not necessarily reflect the official opinion of the European Commission. Neither the European Union institutions and bodies nor any person acting on their behalf, may be held responsible for the use, which may be made of the information contained therein.

Summary and conclusion

The excellent performance and dynamic behaviour for storing electrical energy in hydrogen allow proton exchangeable membrane (PEM) electrolysis to cover the gap between the intermittent renewable power production and the grid demand at different time horizons and scales. However, one of the main hindrance for more wide spread utilisation of PEM-electrolysis is the cost to a certain extent related to the use of noble metals. Lowering the amount of noble metals may jeopardise other features. The presented work concerns the development and characterization of PEM-electrolysis MEAs (membrane electrode assembly) with (ultra) low PGM loading, high performance and low degradation. The specific project targets defined for the MEA development are as follows:

- Reduce the cathode PGM loadings with a factor of >5 down to $\leq 0.1 \text{ mg/cm}^2$
- Reduce anode noble-metal catalyst loading to $\leq 0.4 \text{ mg/cm}^2$
- Demonstrate long-lifetime potential with single cell MEA having a degradation rate of $<5 \text{ } \mu\text{V/h}$
- Achieve a current density of 3 A/cm^2 at 1.8 V/cell and 4.5 A/cm^2 at $E_{\text{Cell}} < 2 \text{ V}$

The work was initiated with a screening analysis carried out at the CNR-ITAE of different MEAs based on various precursors and combinations. The MEAs were judged based on polarisation and EIS; long-term test was performed on selected MEAs with encouraging performance. The project performance targets, with respect to catalyst loading and performance, were obtained for MEAs based on the Solvay membrane Aquivion® E98-09S, stabilised Solvay ionomer (D98-06ASX), and optimised catalysts developed by CNR-ITAE (cathode 40% Pt on C and anode: $\text{Ir}_{0.7}\text{Ru}_{0.3}\text{O}_x$). Information derived from the screening analysis was transferred to EWII in order to scale-up the selected formulations for large scale CCM coating. The activity was thus expanded to cover the ink formulation and processing for the novel ionomers and catalysts. Small, medium and full HPEM2Gas sized MEAs (<10 , 130 and 415 cm^2 active area, respectively) have been manufactured by EWII. The results obtained for the small and the intermediate sized MEAs at ITM are well in line with the results reported by CNR-ITAE.

Long-term test have illustrated that the decay rate declines with time. The lowest performance decay recorded for an optimised HPEM2Gas MEA is $8 \text{ } \mu\text{V/h}$ @ 3 A/cm^2 after $4,000 \text{ h}$ operation, close to the project target. Current and thermal cycling of single cells proved to have limited impact on degradation. Pronounced reversible degradation has been observed at low temperature (55°C) and too a much lower degree at high temperature (80°C).

Table of content

1	Introduction	6
2	Experimental.....	7
2.1	MEA precursors	7
2.2	CCMs and MEAs.....	7
2.3	Single cell test hardware and test protocols	7
3	Single cell test results	10
3.1	Performance and steady state durability results	10
3.2	Operation under Dynamic Conditions.....	13
3.3	Turnover frequency	19
4	3-cell stack test with intermediate sized MEAs	21
5	Post operational characterisation	25

List of acronyms, abbreviations and definitions

Table 1.1 Acronym table

Abbreviation	Explanation
AFC	<u>A</u> dvanced <u>F</u> uel <u>C</u> ell
An	<u>A</u> node
AST	<u>A</u> ccelerated <u>S</u> tress <u>T</u> est
BoL	<u>B</u> eginning- <u>o</u> f- <u>L</u> ife
Cat	<u>C</u> athode
CCM	<u>C</u> atalyst <u>C</u> oated <u>M</u> embrane
CL	<u>C</u> atalyst <u>L</u> ayer
DoA	<u>D</u> escription <u>o</u> f <u>A</u> ction
EC	<u>E</u> lectrolysis <u>C</u> ell
ECSA	<u>E</u> lectro <u>C</u> hemical <u>S</u> urface <u>A</u> rea
EDX	<u>E</u> nergy-dispersive X-ray spectroscopy
EIS	<u>E</u> lectrochemical <u>I</u> mpedance <u>S</u> pectroscopy
EoT	<u>E</u> nd- <u>o</u> f- <u>T</u> est
EW	<u>E</u> quivalent <u>W</u> eight
FC	<u>F</u> uel <u>C</u> ell
GDL	<u>G</u> as <u>D</u> iffusion <u>L</u> ayer
IEA	<u>I</u> nternational <u>E</u> nergy <u>A</u> gency
MEA	<u>M</u> embrane <u>E</u> lectrode <u>A</u> ssemblies
OCV	<u>O</u> pen <u>C</u> ell <u>V</u> oltage
PEMEC	<u>P</u> roton <u>E</u> xchange <u>M</u> embrane <u>E</u> lectrolysis <u>C</u> ell
PFSA	<u>P</u> er <u>F</u> luoro <u>S</u> ulfonic <u>A</u> cid
SEM	<u>S</u> canning <u>E</u> lectron <u>M</u> icroscope
XPS	<u>X</u> -ray photoelectron spectroscopy
XRD	<u>X</u> -ray diffraction

1 Introduction

The HPEM2GAS target is to develop a low cost PEM electrolyser optimised for grid management through both stack and balance of plant innovations, culminating in a six-month field test of an advanced 180–300 kW PEM electrolyser. The present report comprises the results gained after more than two years development activity of the PEM MEAs based on precursors developed within the project. The project target defined for the MEA development comprises the following specific targets:

- Reduce the cathode PGM loadings with a factor of >5 down to $\leq 0.1 \text{ mg/cm}^2$
- Reduce anode noble-metal catalyst loading to $\leq 0.4 \text{ mg/cm}^2$
- Demonstrate long-lifetime potential at high current density with single cell MEA having a degradation rate of $<5 \text{ } \mu\text{V/h}$
- Achieve a current density of 3 A/cm^2 at 1.8 V/cell and 4.5 A/cm^2 at $E_{\text{Cell}} < 2 \text{ V}$

The MEA development has focused on the investigation of the optimal combination of HPEM2Gas catalyst¹ developed by CNR-ITAE, Aquivion® E98-09S membrane, and stabilised Solvay ionomer (D98-06ASX). MEAs were manufactured by EWII by a wet-processing route. The activities were thus expanded to cover the ink formulation and processing for the new ionomers and catalysts developed within HPEM2GAS. Preparation of catalyst inks using wet electrode fabrication routes and involving high-surface catalyst powders was addressed to improve electrochemical characteristics and provide optimal rheology. Screening of the catalyst-ionomer interface was carried out at various partner laboratories to speed-up the materials down-selection process.

The MEA development and manufacturing processes were supported by in-situ and ex-situ methods for characterisation and testing of the inks, electrodes, and MEAs. Special attention was addressed to use the test protocols developed within HPEM2Gas.² A number of techniques such as rheometry, thermal gravimetric analysis, porosimetry, SEM, TEM, XRD, impedance spectroscopy, voltammetry, etc. were used by the project partners for a complete assessment of the MEA properties.

This report summarises the performances obtained and the knowledge gained in particular with respect to MEA durability and degradation.

¹ Cf. HPEM2Gas 'D3.4 Publishable report on catalyst development'

² Cf. HPEM2Gas 'D2.1 Protocols for characterisation of system components and electrolysis system assessment'

2 Experimental

2.1 MEA precursors

Details on the HPEM2Gas catalyst-precursor development is reported in the public deliverable report D3.4.¹ A list of the HPEM2Gas CCM-precursors utilised for the MEA manufacture reported *ibid* is provided in Table 2.1.

Table 2.1 Utilised CCM precursors.

ID	Explanation	Comments
E98-09S	Solvay extruded baseline membrane	Aquivion® E98-09S is a chemically stabilized PFSA ionomer membrane with an EW of 980 g/eq. The E98-09S is 90 µm thick
D83-06A	Solvay ionomer	EW=830 g/eq (baseline ionomer). Dispersion is formulated with propanols and have 6 wt% of polymer content
D83-06ASX	Solvay ionomer	EW=830 g/eq, stabilized ionomer. Dispersion is formulated with propanols and have 6 wt% of polymer content
D87-25BS	Solvay ionomer	EW=870 g/eq, stabilized ionomer. Aqueous ionomer dispersions
D98-25BS	Solvay ionomer	EW=980 g/eq, stabilized ionomer. Aqueous ionomer dispersions
D98-06ASX	Solvay ionomer	EW=980 g/eq, stabilized ionomer. Dispersion is formulated with propanols and have 6 wt% of polymer content
IrRuOxSA	CNR-ITAE anode catalyst	$\text{Ir}_{0.7}\text{Ru}_{0.3}\text{O}_x$ (Ir:Ru = 70:30 atom ratio), crystallite size ≈ 9 nm
Pt/C SS	CNR-ITAE cathode catalyst	30 wt% Pt on carbon 40 wt% Pt on carbon; crystallite size ≈ 3 nm

2.2 CCMs and MEAs

All CCMs are design symmetrically with respect to type of ionomer. Four different ionomers have been tested at three and six levels for the cathode and anode, respectively. The cathode PGM loading has been varied between 0.1-0.6 mg/cm² and the anode PGM loading between 0.25-2.5 mg/cm². The catalyst inks were directly sprayed onto the membranes. Carbon GDL was applied to the cathode.

The manufactured CCM compositions with HPEM2Gas precursors are listed in Table 2.2.

2.3 Single cell test hardware and test protocols

Single cell hardware for the initial screening of various combinations of electrocatalysts and ionomers consisted of ambient pressure cells, differing in terms of active area or operating mode e.g. pressurised or ambient pressure operation. The PEM electrolyser performance was evaluated at different temperatures and under ambient pressure. The applied test protocols are listed in Table 2.3. A significant difference between the test conditions at CNR-ITAE and EWII is the anode water

Table 2.2 Manufactured CCM compositions.

EWII	CNR-ITAE	CCM ID	Cathode			Membrane	Anode		
			Catalyst batch	mg _{Pt} /cm ²	Ionomer		Ionomer	mg _{IrRu} /cm ²	Catalyst batch
X		MEE0036	Pt/C SS01	0.1	D98-06ASX	E98-09S	D98-06ASX	0.40	IrRuOx SA14L
X		MEE0037	Pt/C SS01	0.1	D98-06ASX	E98-09S	D98-06ASX	0.25	IrRuOx SA14L
X		MEE0038	Pt/C SS01	0.1	D98-06ASX	E98-09S	D98-06ASX	0.33	IrRuOx SA14L
X		MEE0039	Pt/C SS01	0.1	D98-06ASX	E98-09S	D98-06ASX	0.84	IrRuOx SA14L
X		MEE0075	Pt/C SS01	0.1	D83-06ASX	E98-09S	D83-06ASX	0.40	IrRuOx SA14L
X		MEE0076	Pt/C SS01	0.2	D83-06ASX	E98-09S	D83-06ASX	1.26	IrRuOx SA14L
X		MEE0077	Pt/C SS01	0.6	D83-06ASX	E98-09S	D83-06ASX	2.51	IrRuOx SA14L
	X	Cell 68	Pt/C SS00	0.1	D83-06AX	E98-09S	D83-06AX	0.34	IrRuOxSA07L
	X	Cell 69	Pt/C SS01	0.1	D83-06AX	E98-09S	D83-06AX	0.34	IrRuOx SA14L
	X	Cell 79	Pt/C SS01	0.1	D83-06AX	E98-09S	D83-06AX	0.34	IrRuOx SA14L
	X	Cell 82	Pt/C SS01	0.1	D98-06ASX	E98-09S	D98-06ASX	0.34	IrRuOx SA14L
	X	Cell 83	Pt/C SS01	0.1	D98-06ASX	E98-09S	D98-06ASX	0.34	IrRuOx SA14L
	X	Cell 84	Pt/C SS01	0.1	D98-06ASX	E98-09S	D98-06ASX	0.34	IrRuOx SA14L
	X	Cell 88	Pt/C SS02	0.1	D98-06ASX	E98-09S	D98-06ASX	0.34	IrRuOx SA16L
	X	Cell 90	Pt/C SS02	0.1	D83-06ASX	E98-09S	D83-06ASX	0.34	IrRuOx SA16L
	X	Cell 91	Pt/C SS02	0.1	D98-06ASX	E98-09S	D98-06ASX	0.34	IrRuOx SA16L

Table 2.3 *Standard single cell test parameters*

Parameter	Unit	CNR-ITAE	EWII	AFC Annex 30
T_{Cell}	°C	80	70	60 (IND) or 80 (R&D)
Anode H ₂ O Flow Temp.	°C	-	70	60 or 80 (inlet)
Cathode H ₂ O Flow Temp.	°C	-	-	60 or 80 (inlet), Optional H ₂ O-flow
H ₂ O Anode Flow	ml/min/cm ²	1	8.6	≥2, $\Delta T \leq 2^\circ\text{K}$
H ₂ O Cathode Flow	ml/min/cm ²	-	-	2 (optional)
P_{An}	Bar(abs)	Ambient	Ambient	1 @ outlet
P_{Cat}	Bar(abs)	Ambient	Ambient	1 @ outlet
Water quality	MΩ·cm	18.2	>0.1	ASTM Type II (>1 MΩ·cm)

flow and purity, in particular the water quality may influence the performance. Anode water is recirculating in the single cell test; the water was maintained at the cell temperature.

Electrochemical measurements, including polarization curves, electrochemical impedance spectroscopy (EIS), galvanostatic durability tests. CNR-ITAE used an Autolab PGSTAT 302 Potentiostat/Galvanostat equipped with a current booster (Metrohm) and FRA (frequency response analyser). Hydrogen concentration in the oxygen stream was monitored by an AGILENT micro GC. EWII used an in-house constructed hard- and software.

The iV polarization curves at CNR-ITAE were recorded by increasing stepwise the cell current according to a specific protocol, reported in D2.1², with a cut-off voltage of 2 V. Electrochemical impedance measurements were carried out at 1.5 V and the frequency varied from 100 kHz to 100 mHz in single sine mode. The amplitude of the sinusoidal excitation signal was 0.01 V. The iV polarization curves at EWII were recorded by first increasing the cell current with 0.09 A/min from 1 mA to 6 A (2.1 A/cm²) followed by a decrease with -0.09 A/min; the cut-off voltage was normally 2 V although it was increased to 2.3 V in special tests.

3 Single cell test results

3.1 Performance and steady state durability results

An initial screening of electrocatalysts (CNR-ITAE), membrane and ionomer (Solvay) formulations was carried out at CNR-ITAE. The different MEAs were screened using steady state durability tests of about 100, 200 and 1,000 hrs at 1 and 3 A cm⁻². Endurance tests of 1,000 hrs at 1 A cm⁻² were applied to the most promising formulations, an example is provide in Fig. 3.1. In the first set of measurements, non-stabilized Aquivion ionomers performed better than stabilized Aquivion ionomers both in term of performance and stability. This result was quite surprising especially with regard to the stability. It was realized successively that this was just related to the MEA manufacturing procedure. Successively, the MEA manufacturing was optimised (Fig. 3.1 & Fig. 3.2).

The cathode formulation based on 40 wt% Pt/C was performing better than that based on 30 wt% Pt/C (the overall Pt loading was kept constant to 0.1 mg cm⁻²), probably because a thinner electrode layer favours hydrogen escape and ease mass-transport. In addition, anode catalyst production in a large batch produced CCMs with slightly better performance and stability. The most appropriate membrane was the stabilized Solvay Aquivion membrane with a 90 µm thickness and 980 EW (Fig. 3.1).

Optimisation of the ink formulation at CNR-ITAE allowed increasing both performance and stability (Fig. 3.3). The recorded performance of 1.82 V at 3 A cm⁻² was essentially equal to the project target of (1.80 V at 3 A cm⁻² with <0.5 mg cm⁻² PGM loading) (Fig. 3.3). This was the result of an appropriate trade-off between electronic and ionic percolations in the catalytic layers and the extension of the reaction interface between the catalyst and the electrolyte.

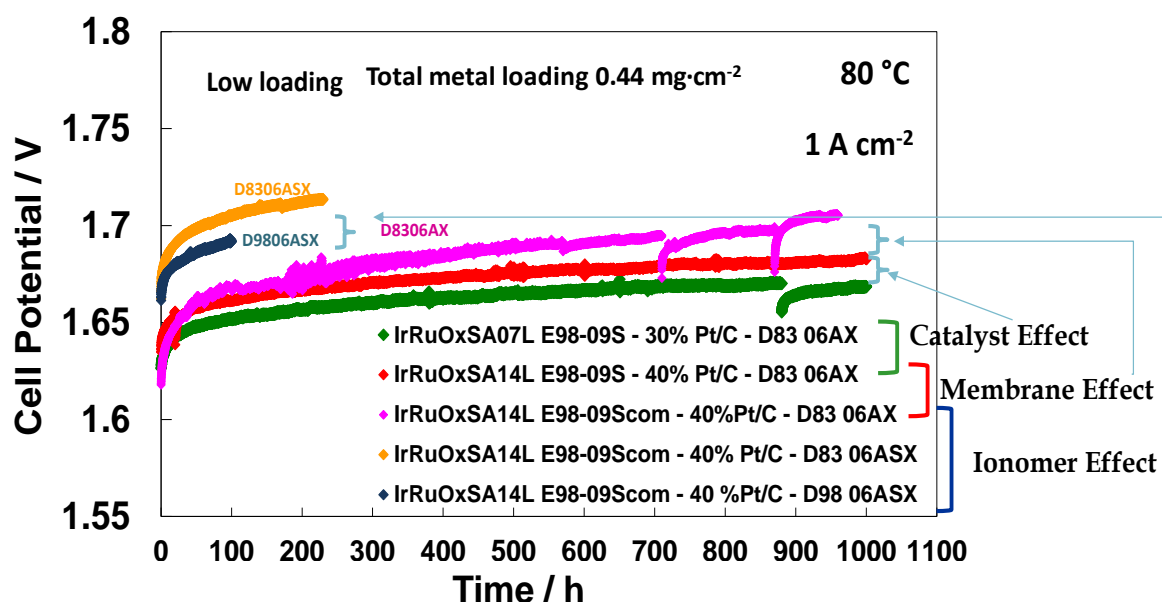


Fig. 3.1 Durability Test at CNR-ITAE at 1 A·cm⁻² and 80°C: Ionomer, Membrane and Catalyst Effects.

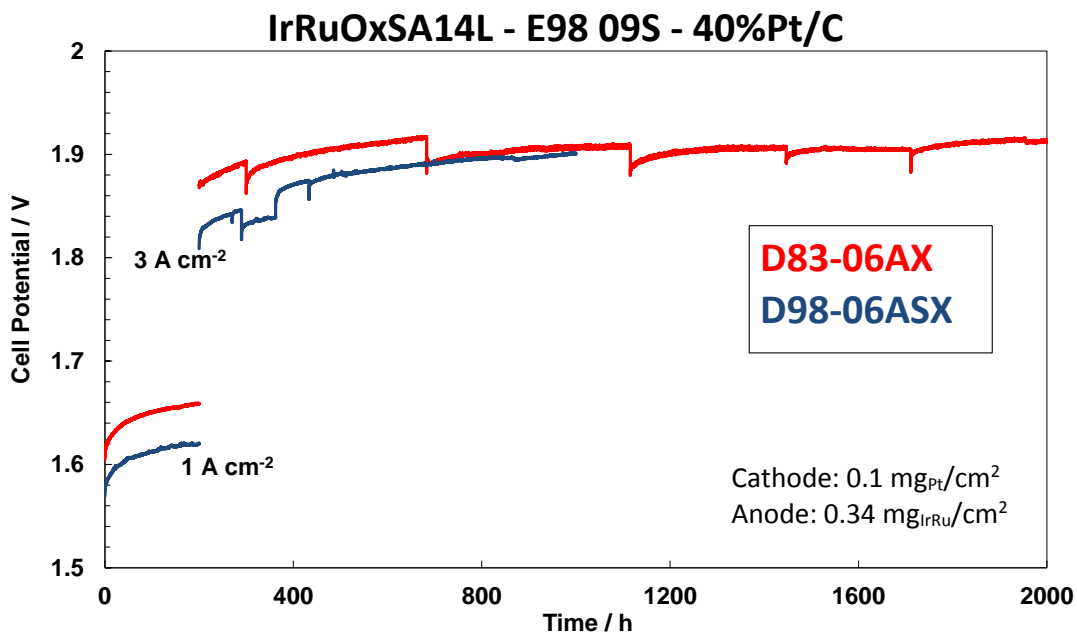


Fig. 3.2
Durability
Test at
CNR-ITAE
at 1-3
A·cm⁻²
and 80°C:
Different
stabilised
Ionomers.

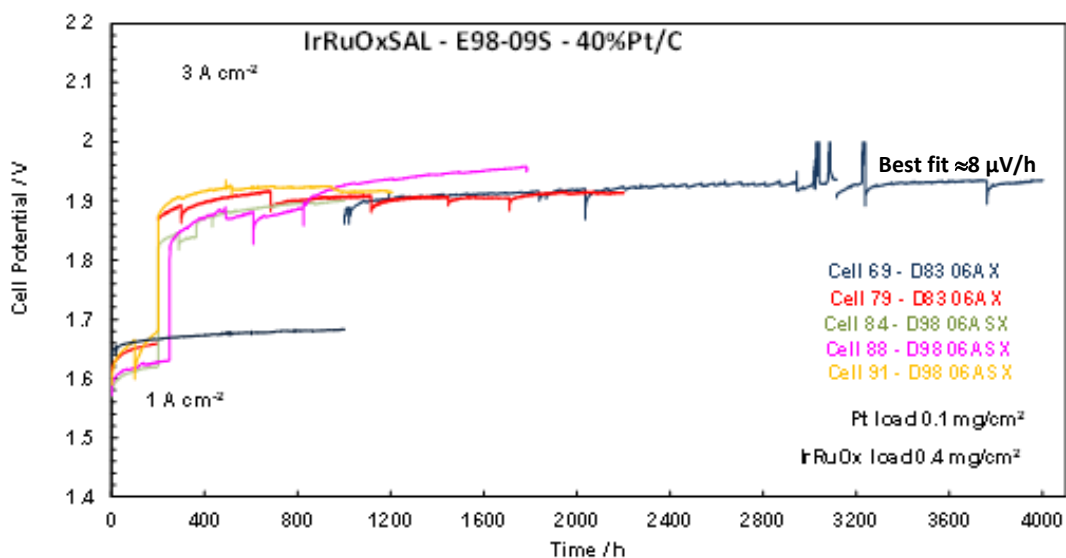


Fig. 3.3
Durability
studies at CNR-
ITAE for
different MEAs
based on non-
stabilised and
stabilised
ionomers at
80°C.

A proper tailoring of the MEA manufacturing was required to achieve improved stability. An excellent stability at both 1 and 3 A cm⁻² for 4,000 h was obtained at CNR-ITAE allowing to achieve the project target (cell 69 cf. Table 2.2).

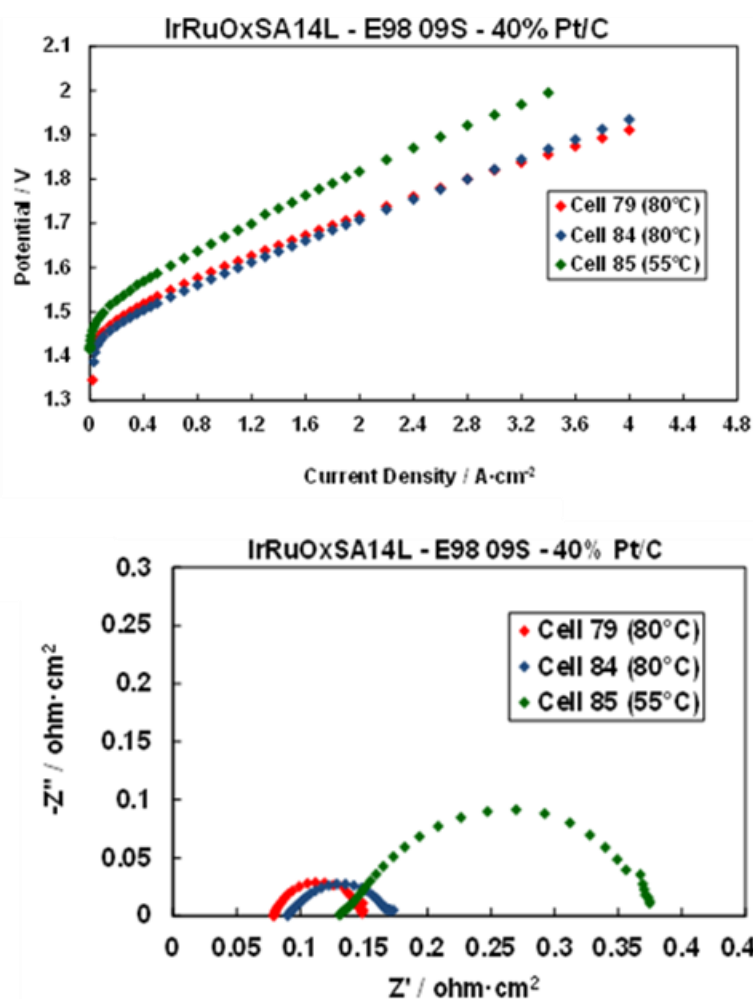


Fig. 3.4
Polarization curves (top)
and Impedance Spectroscopy (bottom)
carried out at CNR-ITAE
at different operating
temperatures: Cell 79
and cell 84 has been
tested in total for 2,000
and 1,000 h's at 1 A·cm⁻²,
respectively, prior to the
shown characterisation.

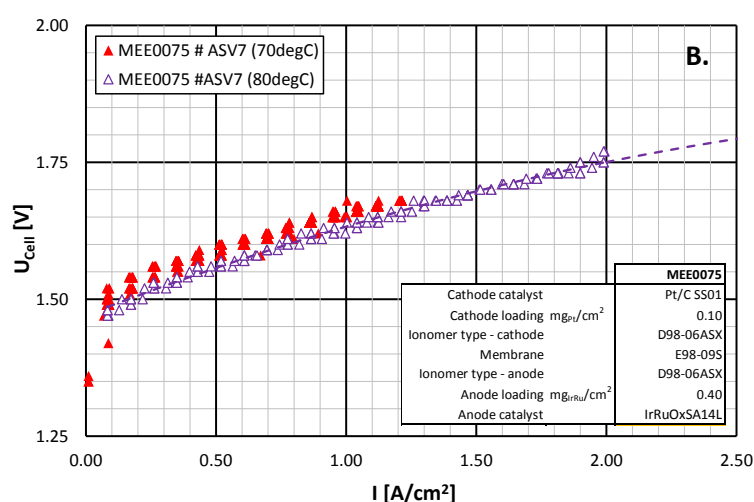
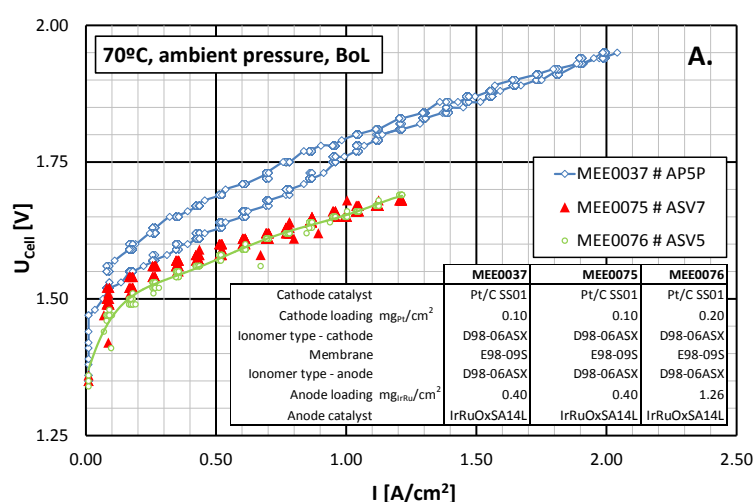
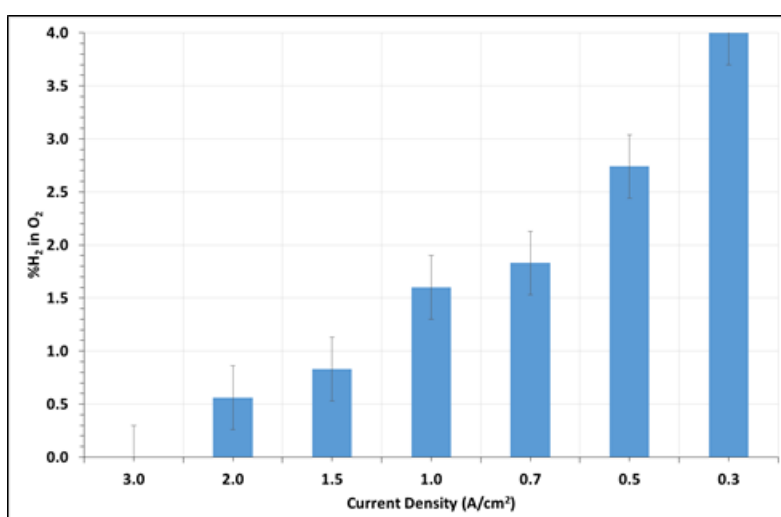


Fig. 3.5 CCM performance of optimised MEAs at EWII prepared by spray coating.

The effect of the operating temperature is evident in the polarisation curves and AC-impedance spectra in Fig. 3.4 showing an increase of series resistance (ohmic resistance), mass transport constraints and activation losses passing from 80°C to 55°C.



*Fig. 3.6
%H₂ in O₂ at 54°C, 20 bar H₂
pressure, measured during
testing of a ≈ 1.5 mg_{PGM}/cm²
PGM loaded CCM,
manufactured by EWII.*

The manufacture of selected MEA formulations has successfully been scaled up from MEAs <10 cm² to full size HPEM2Gas MEAs (415 cm²) by EWII (Fig. 3.5). The effect of MEA optimisation is visible in Fig. 3.5A where the CCMs with optimised ionomer content shows no hysteresis. The temperature effect is less pronounced in these results (Fig. 3.5B) perhaps because this effect is masked by using less pure feed water cf. Table 2.3.

Measurement of the %H₂ in O₂ during operation at high differential pressure and different current densities was carried out using an electrochemical sensor (HyOptima 720, minimum level of detection 0.4%, 0.3% accuracy) placed within the exhaust vent of the O₂ vent line. Measurement was conducted whilst testing a CCM with intermediate PGM loading (Fig. 3.6). The %H₂ in O₂ was below 2% within the current density range 0.7–3 A/cm² (23%–100% load); at nominal current density of the demonstration system (3 A/cm²) it was below the level of detection.

3.2 Operation under Dynamic Conditions

A current density (load) cycling single cell test was performed at both ITM and CNR-ITAE. At CNR-ITAE, it was observed that decreasing operating potential window periodically can mitigate cell degradation, although this might be solely reversible degradation. No relevant influence was observed in thermal cycles.

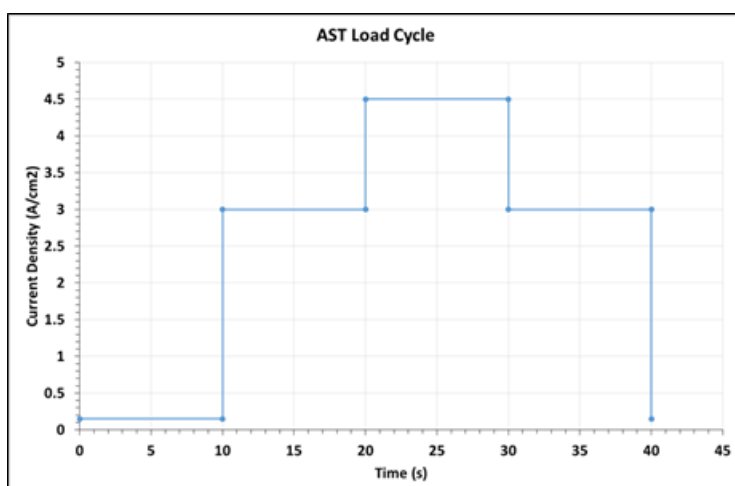


*Fig. 3.7
Accelerated stress test load profile
at ITM.*

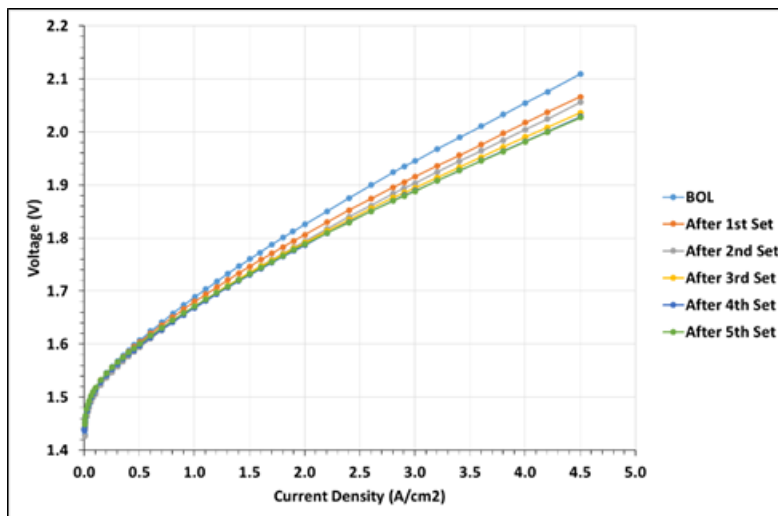


*Fig. 3.8
Polarisation curves at 54°C,
ambient pressure, for a ≈ 1.5
 $\text{mg}_{\text{PGM}}/\text{cm}^2$ PGM loaded CCM
in a water electrolysis cell
during AST cycle testing (ITM).*

In the field, the demonstration system will be subject to a variation in load and On/Off cycles, therefore the various CCMs were subjected to different types of accelerated stress test (AST) at ITM. In the first test, the load was varied between 5% ($0.15 \text{ A}/\text{cm}^2$) and 150% ($4.5 \text{ A}/\text{cm}^2$) of the nominal current density. The cell was subjected to five sets of 1,500 cycles of the load profile shown in Fig. 3.7, controlled by a potentiostat.

Unfortunately, it was found that the low PGM loading CCM was unable to be tested under these conditions, as the cell voltage reached the cut-off voltage of 2.2 V, before reaching $4.5 \text{ A}/\text{cm}^2$. The intermediate PGM loading CCM was able to be tested, however and found to be relatively stable. To measure the durability, the cell voltage increase associated with cell decay was determined from polarisation curves measured before and after each set of 1,500 cycles, at 1 and $3 \text{ A}/\text{cm}^2$. The performance decay was reported as %-loss of voltage efficiency at the specific currents (Fig. 3.8 & Table 3.1).

Table 3.1 Voltage efficiency and loss of efficiency during the AST cycle testing of a $\approx 1.5 \text{ mg}_{\text{PGM}}/\text{cm}^2$ PGM loaded CCM with improved hot-pressing, manufactured by EWII.

Cycle	Voltage Eff. (%)		% Voltage Eff. Loss	
	1 A/cm^2	3 A/cm^2	1 A/cm^2	3 A/cm^2
BoL	87.6	76.1	-	-
1	88.1	77.2	-0.5	-1.2
2	88.6	77.8	-1.0	-1.7
3	88.5	78.1	-0.9	-2.0
4	88.7	78.3	-1.1	-2.3
5	88.5	78.4	-0.9	-2.3

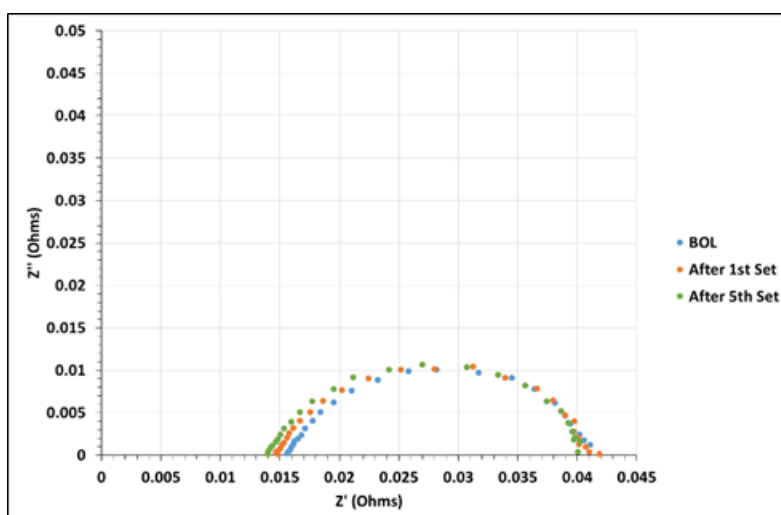


*Fig. 3.9
AC impedance spectroscopy
for $\approx 1.5 \text{ mg}_{\text{PGM}}/\text{cm}^2$ PGM
loaded CCMs with improved
hot-pressing, manufactured by
EWII, measured during AST
cycle testing at $0.1 \text{ A}/\text{cm}^2$
(ITM).*

The voltage efficiency was actually found to gradually improve with each set of 1,500 cycles, particularly at high current density. AC impedance showed that there was a slight decrease in series resistance and an increase in polarisation resistance when compared against the BoL, first set and final set of 1,500 cycles (Fig. 3.9). This trend was also observed with the high PGM loading CCMs.

The intermediate PGM loading CCM was also subjected to an ITM in-house designed accelerated stress test in order to validate the durability of the catalyst layers during On/Off cycling, mimicking real life operation. A novel PEMWE design had previously been developed in partnership with the National Physical Laboratory (NPL).³ The cell design contains a luggin capillary connected to a reference electrode, and is engineered so that when it is operational there is intimate contact made between the MEA and the capillary allowing for the overall cell voltage to be split into the potential contributions of the anode and cathode (Fig. 3.10).

The reference electrode-electrolyser cell has been used to better understand the electrolyser. For example, it can be used to measure the electrochemically active surface area of the electrodes. In using the cell it was found that when a cell is turned off (OCV), the cell voltage gradually falls to 0 V, as the cell discharges, but looking at the individual electrode potentials, it is the potential of the cathode that changes significantly, rising to meet the potential of the anode; the change in the anode potential is relatively small (Fig. 3.11). This change in potential puts a considerable stress on the

³ E. Brightman, J. Dodwell, N. van Dijk, G. Hinds, *Electrochemistry Communications*, 2015, 52, 1.

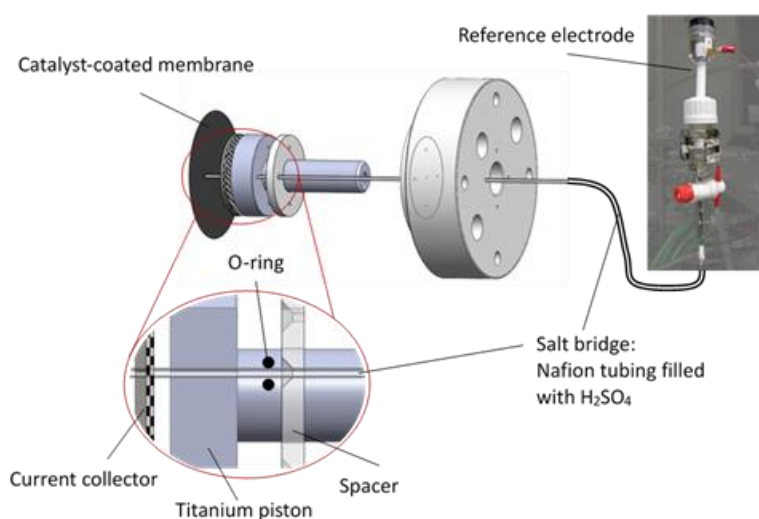


*Fig. 3.10
Reference electrode integration
into the small-scale ITM Power
PEMWE design.*

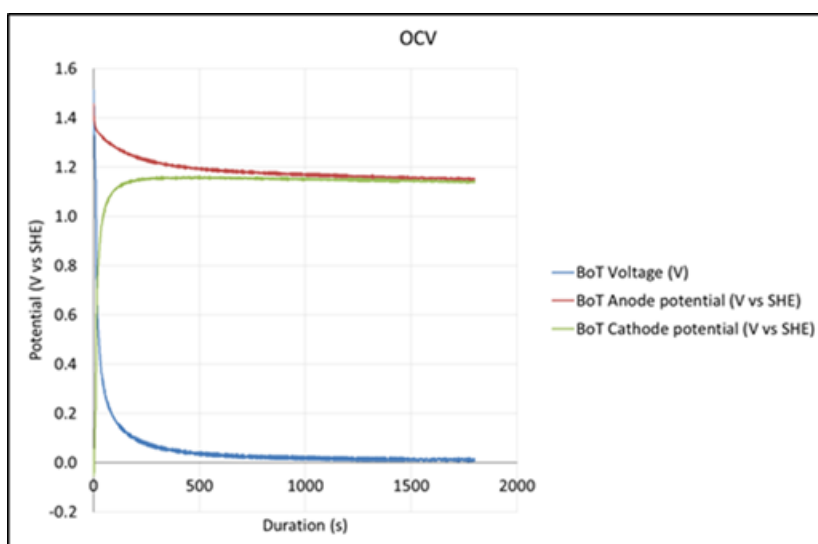


*Fig. 3.11
Behaviour of the cell
voltage and anode and
cathode potentials versus a
standard hydrogen
electrode, at open circuit
potential, immediately
after current has stopped
flowing (ITM).*

cathode electrode and has been found to result in the loss of cathode catalyst surface area. Using this knowledge a voltage-controlled AST for power cycling was created replicating many On/Off cycles.

A cell containing the intermediate PGM loading CCM was connected to a potentiostat and the cell voltage was cycled between 1.7 V (Cell On) and 0 V (Cell Off) every 60 s. The test was carried out at 54°C, ambient pressure for a total of 4,000 On/Off cycles. To measure the durability during the test, the cell voltage increase associated with cell decay was determined from polarisation curves measured before and after each set of 1,000 cycles at 1 A/cm². The performance decay was reported as %-loss of voltage efficiency (Fig. 3.12, Table 3.2).

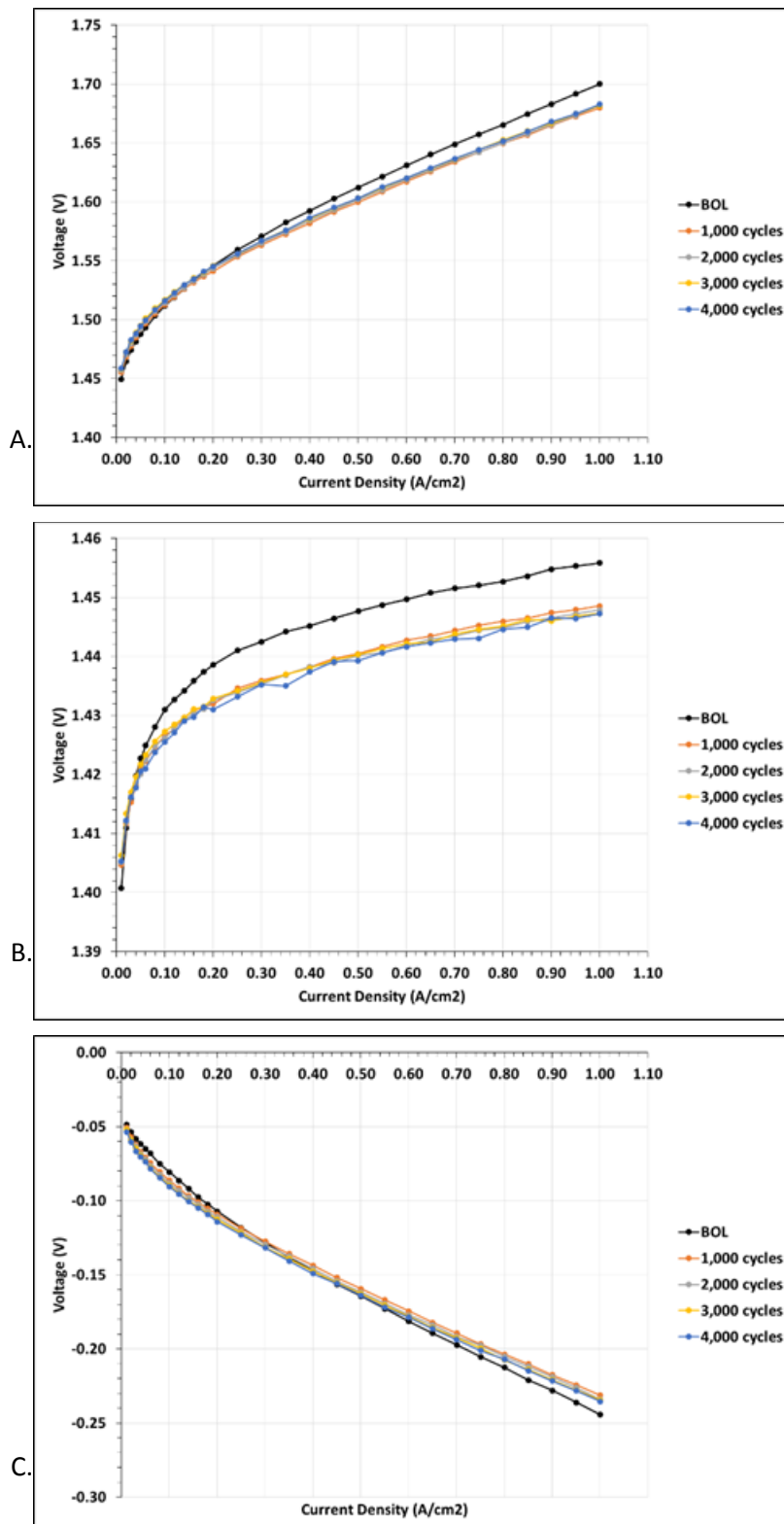


*Fig. 3.12
Polarisation curves at ITM at 54°C, ambient pressure, for a $\approx 1.5 \text{ mg}_{\text{PGM}}/\text{cm}^2$ PGM loaded CCM with improved hot-pressing, manufactured by EWII, during AST cycle testing using the reference electrode-electrolyser cell.
A) Cell, B) Anode & C) Cathode.*

Table 3.2 Voltage efficiency and loss of efficiency during the AST cycle testing using the reference electrode-electrolyser cell, of a $\approx 1.5 \text{ mg}_{\text{PGM}}/\text{cm}^2$ PGM loaded CCM with improved hot-pressing, manufactured by EWII.

Cycles	Voltage Eff. (%)	% Voltage Eff. Loss
BoL	87.1	-
1,000	88.1	-1.1
2,000	88.0	-0.9
3,000	88.0	-0.9
4,000	87.9	-0.9

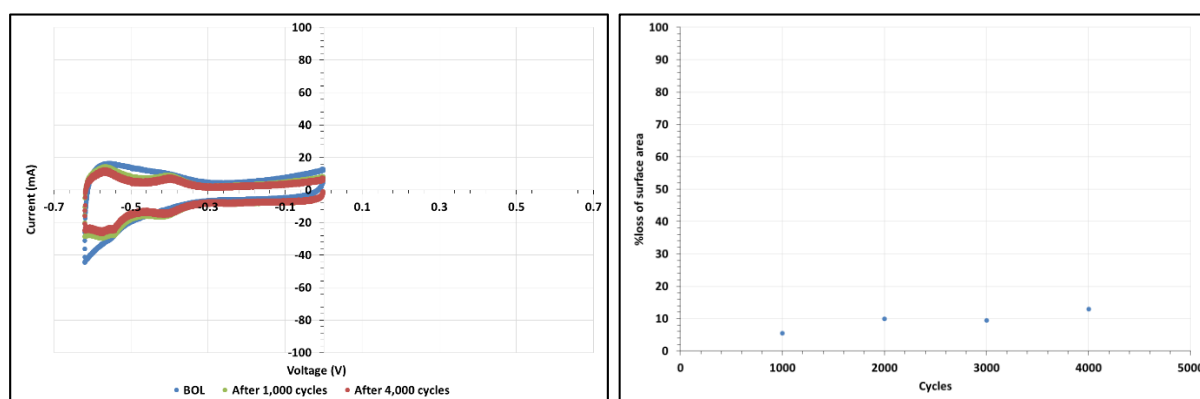


Fig. 3.13 Cyclic voltammogram measured at the beginning of life (BoL), 1,000 hrs and 4,000 hrs (left) and %loss of surface area of the cathode catalyst (right) during AST cycle testing using the reference electrode-electrolyser cell, of a $\approx 1.5 \text{ mg}_{\text{PGM}}/\text{cm}^2$ PGM loaded CCM with improved hot-pressing, manufactured by EWII.

As in the other cycling test, the voltage efficiency actually improved compared to the BoL. From the data collected, both the anode and cathode show an improvement in potential, resulting in an overall lowering of the cell voltage (Fig. 3.12A). The anode is responsible for the majority of this improvement, which takes place over the first set of 1,000 cycles (Fig. 3.12B). Over the following 3,000 cycles, the anode continues to show very gradual improvement, whereas the cathode potential gradually becomes more cathodic (Fig. 3.12C).

The electrochemical surface area of the cathode catalyst was measured using cyclic voltammetry (Fig. 3.13). The loss of cathode surface area was used as a measure of the durability of the CCM to intermittent operation. During the first set of 1,000 cycles, the hydrogen adsorption and desorption peaks in the cyclic voltammogram become more defined compared to the beginning of life. After 4,000 cycles the electrochemical active surface area shows a small decrease ($\approx 13\%$ loss of surface area, Table 3.2).

In conclusion, under dynamic conditions applied at ITM, a cell with intermediate PGM loading CCMs showed good stability during several 1,000 On/Off cycles and cycles between 5% and 150%, at $\approx 55^\circ\text{C}$. The voltage efficiency was actually found to gradually increase as a result of load and On/Off cycling. The improvement in efficiency may in part be due to an adaptation of the CCM topology to the rough surface of the cell's porous diffusion layers.

Based on this data and the data collected under stationary conditions, the intermediate catalyst loading CCMs would be the preferred option for the electrolyser stack of the demonstration system, as it provides the best compromise between a reduction in catalyst loading from the current state of the art (50% reduction in PGM loading) and performance.

3.3 Turnover frequency

The effect of catalyst loading and operating current density was investigated at CNR-ITAE. The degradation rate in Fig. 3.14 was estimated from the linear fitting of the voltage increase during the entire test but excluding the first 100 h that can be considered a typical conditioning period where reversible degradation essentially due to mass transport constraints is prevailing. Whereas a test of 1,000 h represents the minimum operating period to make an estimation of the lifetime of the electrolysis system. Fig. 3.14a shows the cell endurance tests for the MEA with low anode catalyst loading ($0.34 \text{ mg}_{\text{IrRuOx}}/\text{cm}^2$). The cell potentials at the beginning of each experiment for the two operating current densities, 1 A/cm^2 and 3 A/cm^2 , were 1.65 V and 1.85 V, respectively. The degradation rate was $15 \text{ } \mu\text{V/h}$ at 1 A cm^{-2} and increased to $23 \text{ } \mu\text{V/h}$ at 3 A/cm^2 . Thus, there was a significant effect of the operating current density/cell voltage on performance degradation. The degradation rate increased however less than twice with a three-fold increase of current load. The same experiment was repeated with another MEA prepared with much larger anode catalyst loading, i.e. 1.27 mg/cm^2 (Fig. 3.14b). The cell potentials at the beginning of each experiment for the two operating current densities, 1 A/cm^2 and 3 A/cm^2 , were 1.6 V and 1.8 V, corresponding to an enthalpy efficiency of about 90% and 80%, respectively⁴. Thus, the operating potential was roughly 50 mV lower than for the previous MEA for each current load condition. The degradation rate was significantly lower for the high catalyst loading MEA i.e. $5 \text{ } \mu\text{V/h}$ at 1 A/cm^2 and increased to only $11 \text{ } \mu\text{V/h}$ at 3 A/cm^2 (Fig. 3.14b). It is observed that the cell with higher catalyst loading operating at about 1.8 V at 3 A/cm^2 showed slightly lower degradation rate than the cell with lower catalyst loading operating at 1.65–1.7 V at lower current density (1 A/cm^2). Thus, according to these results, the low catalyst loading appears to play a role more relevant than the cell potential in determining the degradation rate ($\mu\text{V/h}$). Since the anode catalyst loading was decreased almost four times in these experiments (from 1.27 mg/cm^2 to 0.34 mg/cm^2) the corresponding increase of the corrosion rate appears to be related more to the increase of the turn-over frequency than to the operating potential window.⁵ Therefore, the large increase of degradation rate at low catalyst loading under operation at 3 A/cm^2 is very likely produced by the strong increase of turnover frequency. A progressive increase of the degradation rate with the turnover frequency, here reported as mass-normalized electrolysis current (A/g), is observed in Fig. 3.15a. A possible explanation of this phenomenon could be searched into the amount of heat that is released per unit of time and amount of catalyst loading (i.e. per catalytic site) during operation. The electrolysis process is exothermic above the thermoneutral potential; thus, the amount of thermal power produced per unit amount of catalyst loading can be obtained from the following formula:

$$W_{\text{th}} = (E_{\text{Cell, in}} - E_{\text{th}}) \cdot I / m_{\text{Cat}}; W_{\text{th}} \equiv W \text{ mg}^{-1}$$

where W_{th} is the thermal power produced per unit amount of catalyst loading, E_{Cell} is the initial operating cell potential at the specific current density, E_{th} is the thermoneutral potential (1.47 V at 80°C)⁴, I is the current density, m_{Cat} is the catalyst mass loading normalized per electrode geometric area. Fig. 3.15b shows a relationship between corrosion rate and heat released per unit of time and amount of catalyst. The trend is similar to that observed between degradation rate and turnover frequency in Fig. 3.15a. Although the limited number of experiments (every test is lasting 1,000 h) carried out does not allow definitive considerations, very likely the local heat produced by the electrochemical exothermic process can cause particle-sintering, growth, dissolution etc. This justifies the increase of the degradation rate with the increase of current density and the decrease of

⁴ P. Millet, N. Mbemba, S.A. Grigoriev, V.N. Fateev, A. Aukauloo, C. Etievant, Int. J. Hydrogen Energy 36 (2011) 4134–4142

⁵ Siracusano, S., Hodnik, N., Jovanovic, P., Ruiz-Zepeda, F., Šala, M., Baglio, V., Aricò, A.S. New insights into the stability of a high performance nanostructured catalyst for sustainable water electrolysis (2017) Nano Energy, 40, pp. 618-632

catalyst mass loading. Whereas, less relevant appears the effect of the operating potential window. Although an increase of corrosion rate with the increase of cell potential is expected, this trend can be masked by the prevailing role of the increased turn over frequency and the effect of the corresponding heat released during operation.

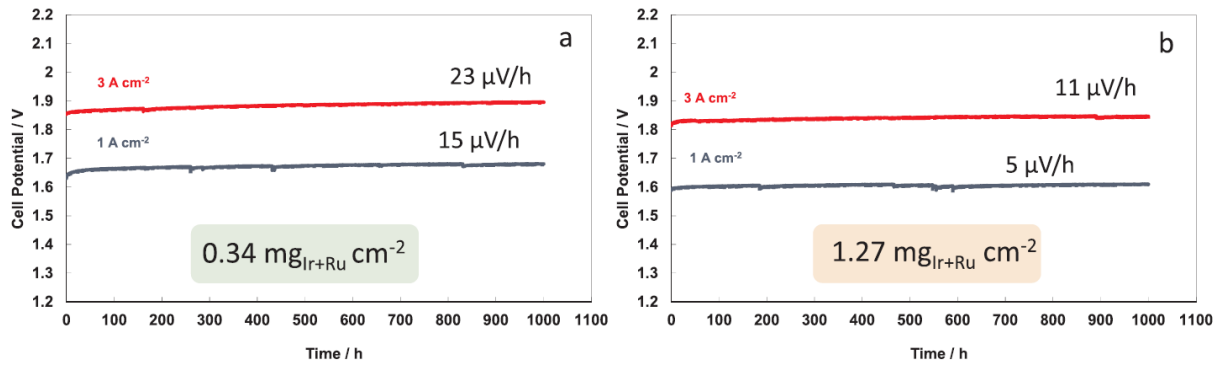


Fig. 3.14 Steady-state durability test at 1 and 3 A/cm² for low (a) and medium (b) anode catalyst loaded MEAs cf. Table 2.3. The cathode catalyst loading is 0.2 mg_{Pt}/cm² for all four MEAs.

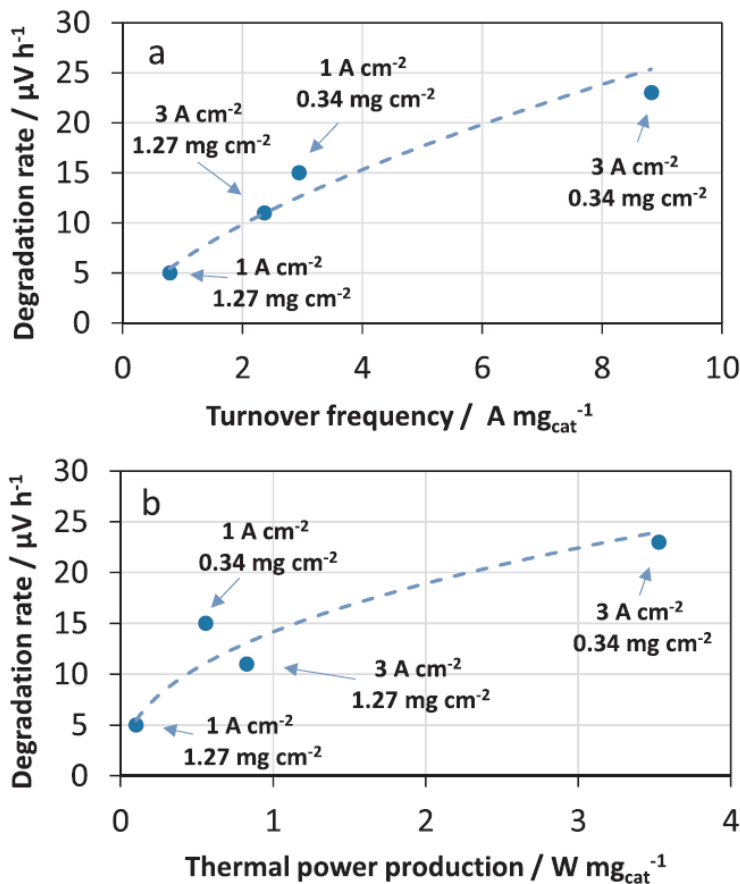


Fig. 3.15 Variation of the degradation rate for the electrolysis cells shown in Fig. 3.14 with different anode catalyst loading and operated for 1,000 hours at different current densities as a function of the turnover frequency (a) and thermal power output (b).

4 3-cell stack test with intermediate sized MEAs

In order to save time and reduce the burden of testing, steady state, constant current tests were conducted at ITM with an intermediate scale 3-cell stack (130 cm² active area). Tests were conducted at 55°C, at differential pressure (H₂ at 20 bar, O₂ at ambient), mirroring the operating conditions of the final demonstration system. The behaviour of the CCMs in the stack was similar to that in the small-scale test cell, in that the stack with the low PGM loaded CCMs had a higher operating voltage than a stack with intermediate PGM loaded CCMs (Fig. 4.1).

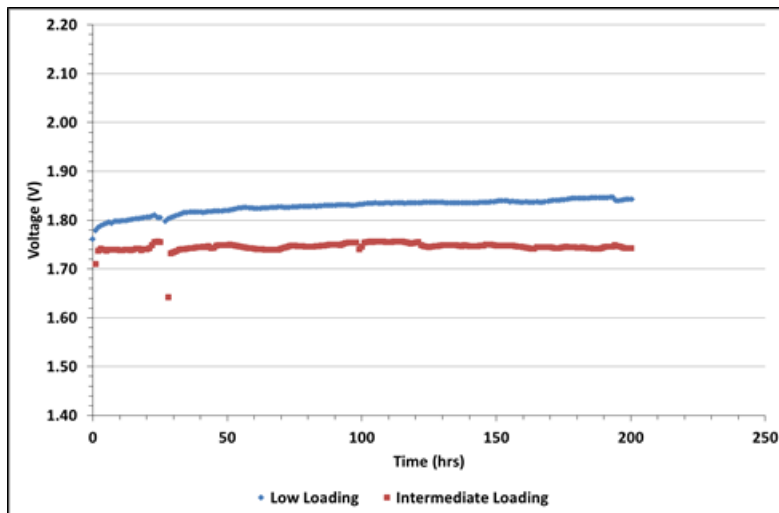


Fig. 4.1
Durability test at 1 A/cm², at 54°C, 20 bar, for different PGM loaded CCMs, manufactured by EWII, in a 3-cell water electrolysis stack.

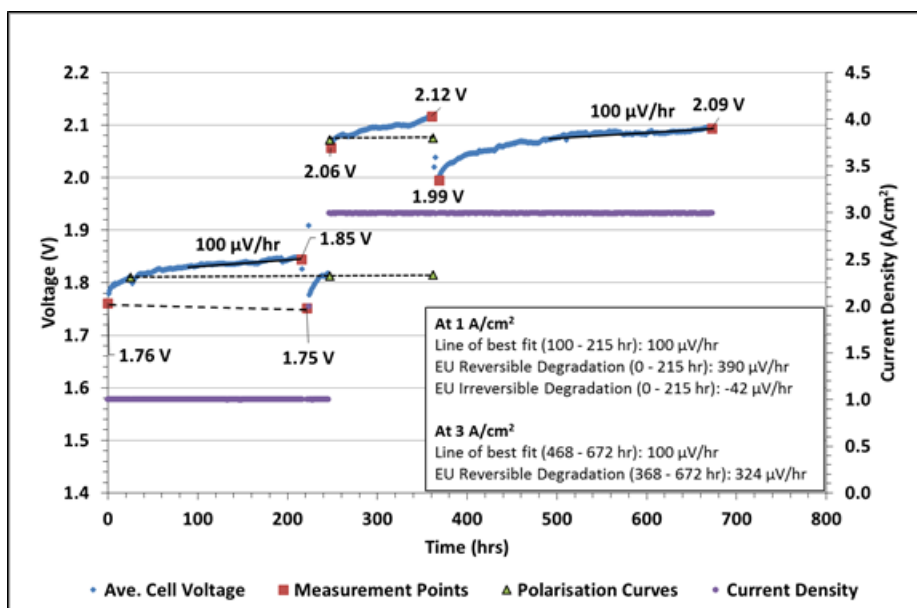
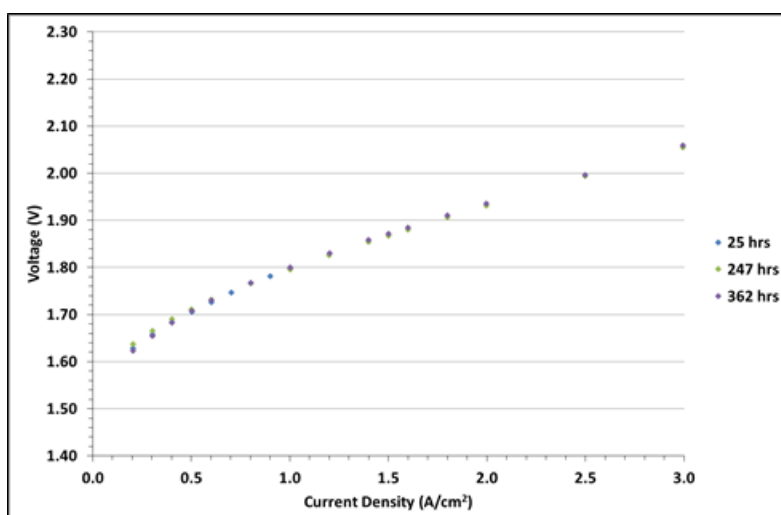


Fig. 4.2
Durability test at different current densities, at 54°C, 20 bar, for ≈0.5 mg_{PGM}/cm² PGM loaded CCMs, manufactured by EWII, in a 3-cell water electrolysis stack.



*Fig. 4.3
Polarisation curves at 54°C, 20 bar pressure, for ≈ 0.5 $\text{mg}_{\text{PGM}}/\text{cm}^2$ PGM loaded CCMs, manufactured by EWII, in a 3-cell water electrolysis stack.*

As before, the voltage degradation was also found to be higher, with a major part of it reversible (Fig. 4.2). The reversible voltage degradation, as defined in the EU draft report on a harmonised set of protocols, after 215 hr of operation, at $1 \text{ A}/\text{cm}^2$, was $390 \mu\text{V}/\text{hr}$, whereas the irreversible degradation was $-42 \mu\text{V}/\text{hr}$.

The HPEM2Gas Milestone 4 durability target of $5 \mu\text{V}/\text{hr}$ at $3 \text{ A}/\text{cm}^2$, is for irreversible degradation. Unfortunately, it was not possible to calculate this as the stack developed a hydrogen crossover issue and the test was stopped after 672 hrs of operation. However, during testing, several polarisation curves were measured showing very little degradation in performance up to $3 \text{ A}/\text{cm}^2$ (Fig. 4.3). Polarisation curves measured at 247 hrs and 362 hrs after a test stoppage show very little variation from that measured after 25 hrs. Based on this data, the voltage degradation at $1 \text{ A}/\text{cm}^2$ was $16 \mu\text{V}/\text{hr}$ (measured between 25-362 hrs) and at $3 \text{ A}/\text{cm}^2$ was $27 \mu\text{V}/\text{hr}$ (measured between 247-362 hrs).

As referred to above, Rozaina et al.⁶ postulated that the percolation of individual anode catalyst particles becomes problematic and electrochemical performances tend to degrade rapidly, below a threshold catalyst loading, leading to poor electrical conductivity within the active layer. This would lead to an increase in localised heat generated by the electrochemical exothermic process at the interface between the catalyst and membrane, which could lead to an increase in ionomer degradation. Work carried out by CNR-ITAE in HPEM2Gas appeared to indicate that catalyst loading and in particular, the turnover frequency plays a more relevant role than the cell potential in determining the degradation rate ($\mu\text{V}/\text{h}$)⁷. The relationship between the corrosion rate and heat released per unit of time and amount of catalyst is similar to that observed between voltage degradation rate and turnover frequency.

The cell voltage of the 3-cell stack tests (intermediate scale), was found to be lower than the single cell tests (small-scale), particularly at higher current density ($>2 \text{ A}/\text{cm}^2$), indicating possible limitations with the design of the small-scale test cell at very high current densities (Fig. 4.4). At $\approx 80^\circ\text{C}$, the performance comes close to the Milestone 3 performance targets of the project for an MEA with a PGM loading of $\leq 0.5 \text{ mg}/\text{cm}^2$. At $3 \text{ A}/\text{cm}^2$, the average cell voltage was 1.89 V ; at $4.5 \text{ A}/\text{cm}^2$ the average cell voltage was 2.02 V . The performance of the intermediate loading CCMs, was even closer to the voltage target, achieving 1.85 V at $3 \text{ A}/\text{cm}^2$ and 2.02 V at $4.5 \text{ A}/\text{cm}^2$. It is interesting

⁶ C. Rozaina, E. Mayousse, N. Guilleta, P. Millet, Applied Catalysis B: Environmental, 2016, 182, 153

⁷ Further elaborated on p. 21, *ibid*.

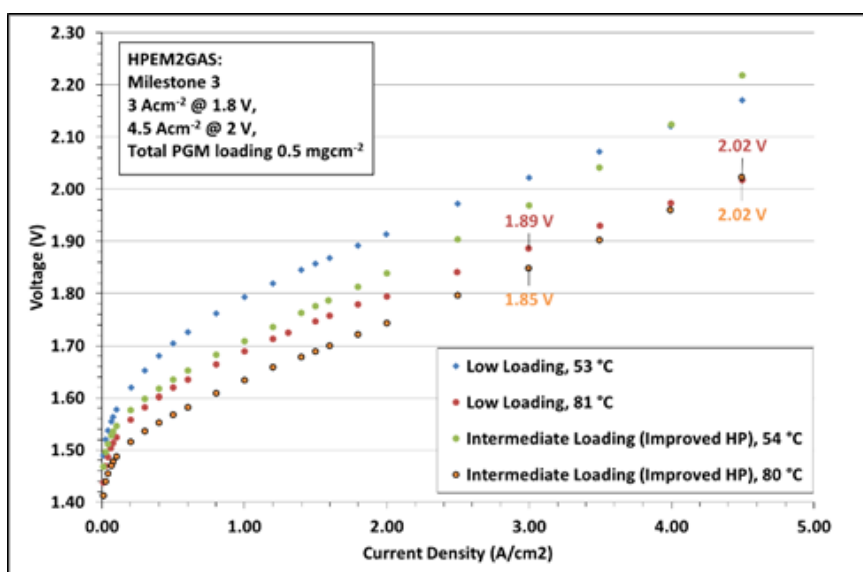


Fig. 4.4
Polarisation curves of average cell voltage at 53-54°C and 80-81°C, ambient pressure, for different PGM loaded CCMs, manufactured by EWII, in a 3-cell water electrolysis stack.

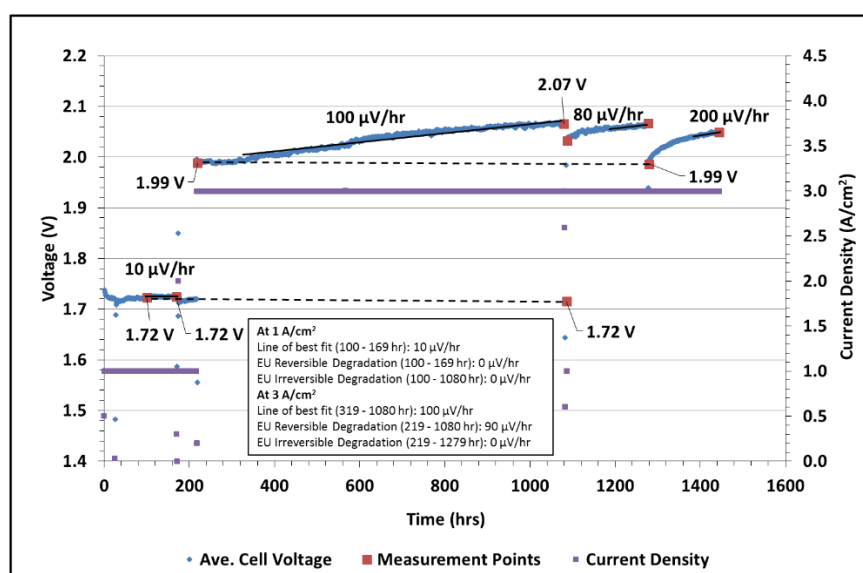
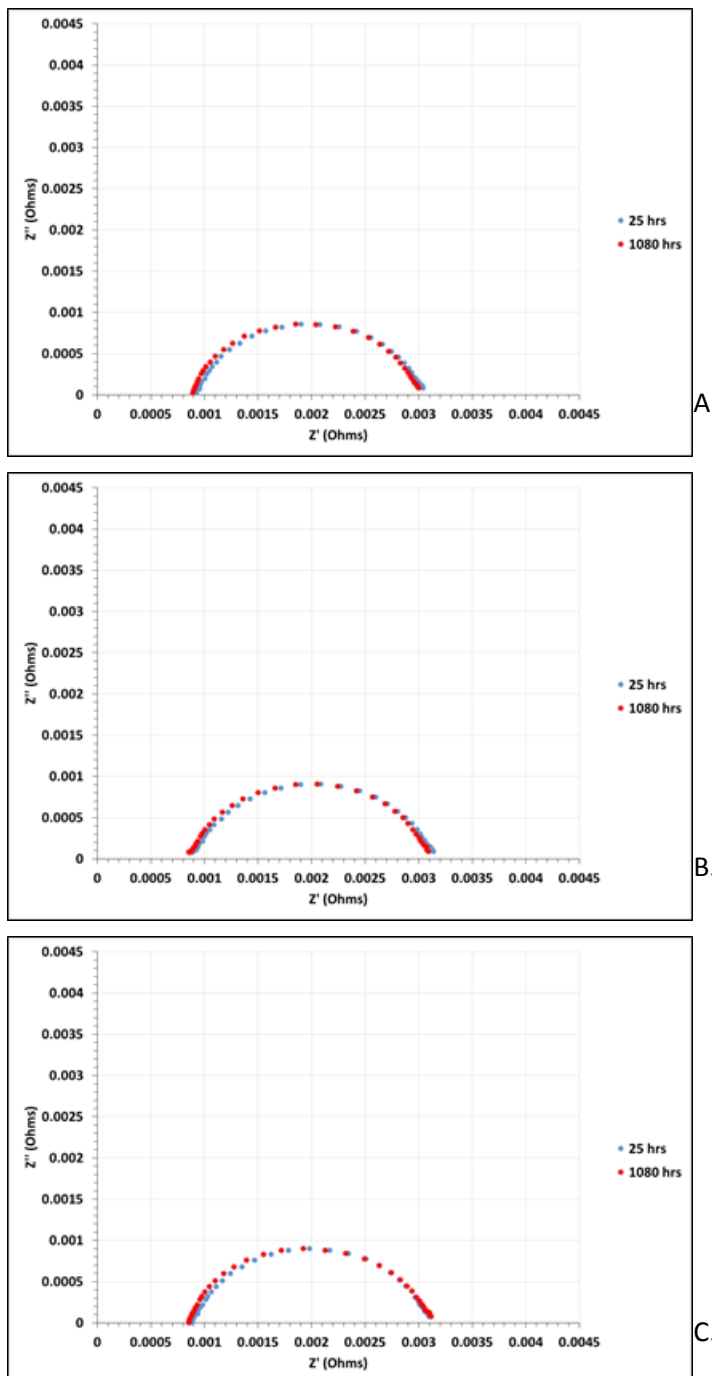


Fig. 4.5
Durability test at different current densities, at 54°C, 20 bar, for ~1.5 mg_{PGM}/cm² PGM loaded CCMs in a 3-cell water electrolysis stack.

to note that at very high current density (>4 A/cm²), the average cell voltage of the stack with the intermediate PGM loading CCMs is similar to that of the stack with the low PGM loading CCMs. A reason for this could be related to the thickness of the catalyst layer. A higher loaded layer would be thicker and is therefore expected to have a higher ohmic resistance.

Durability testing of the intermediate PGM loading CCMs was more successful and lasted close to 1,500 hrs; over 1,200 hrs was at 3 A/cm² (Fig. 4.5). Some reversible voltage degradation was observed, more so when operating at 3 A/cm² than 1 A/cm². During the relatively short time the stack was operated at 1 A/cm², the reversible voltage degradation was calculated to be ~0 μV/hr, using the EU definition and 10 μV/hr, using the line of best fit approach. The irreversible voltage degradation calculated over close to 1,000 hrs was also calculated to be ~0 μV/hr. At 3 A/cm², the reversible voltage degradation was calculated to be 90 μV/hr, using the EU definition and 100 μV/hr using the line of best fit approach. The irreversible voltage degradation over 1,000 hrs was also calculated to be ~0 μV/hr.

A comparison of the AC impedance of the stack measured at 25 hr and 1,080 hr showed very little change in the series and polarisation resistance, providing further evidence that minimal degradation of the catalyst layer had occurred during the test (Fig. 4.6).



*Fig. 4.6
AC impedance spectroscopy for
 $\approx 1.5 \text{ mg}_{\text{PGM}}/\text{cm}^2$ PGM loaded
CCMs with improved hot-
pressing, manufactured by EWII,
in a 3-cell stack at $0.1 \text{ A}/\text{cm}^2$.
A) Cell 1, B) Cell 2 & C) Cell 3.*

In conclusion, under stationary conditions, a stack with intermediate PGM loading CCMs showed greater stability under the operating conditions of the demonstration system ($\approx 55^\circ\text{C}$, 20 bar), when operating at nominal current density ($3 \text{ A}/\text{cm}^2$) and was more efficient (1.85 V, 80% eff, at 80°C , ambient pressure) than a stack with the lower PGM loading CCMs (1.89 V, 78% eff, at 80°C , ambient pressure).

Based on this data and that obtained by CNR-ITAE during Task 4.1, the intermediate catalyst loading CCMs would be the preferred option for the electrolyser stack of the demonstration system, as it provides the best compromise between a reduction in catalyst loading from the current state of the art (50% reduction in PGM loading) and performance.

5 Post operational characterisation

CNR-ITAE received two (2) MEAs from ITM based on Aquivion E98-09S membrane: MEE0081 (Low loading): FRESH and USED. The tested MEA was used in a 3-cell stack test (130 cm² active area). The stack was operated at 1 A/cm² for ≈200 hrs and at 3 A/cm² for ≈472 hrs at 54°C, 20 bar (Fig. 5.1). The EoT MEA analyses were conducted by CNR-ITAE on the cell operated at 2 V with a current density of 3 A cm⁻², red line, in Fig. 5.1a. The MEA samples characterized at CNR-ITAE are reported in Fig. 5.1b.

The XRD analysis indicated a slight decrease of crystallite size for the anode (in the range of the experimental error) (Fig. 5.2). The MEA was analysed with the anode side exposed to the X-rays. The ionomer peak is less intense in the fresh than in the used sample. In the case of an anode thinning, one would expect such increase in ionomer peak as due to the membrane contribution. However, no real conclusions can be drawn from this analysis since some loss of catalytic layer could have occurred as consequence of mechanical erosion during dismantling. As reported in the HPEM2Gas delivery report D3.1, after the durability test, the anode layer appears to be less agglomerated than at the beginning due to an infiltration of ionomer in to the agglomerate.

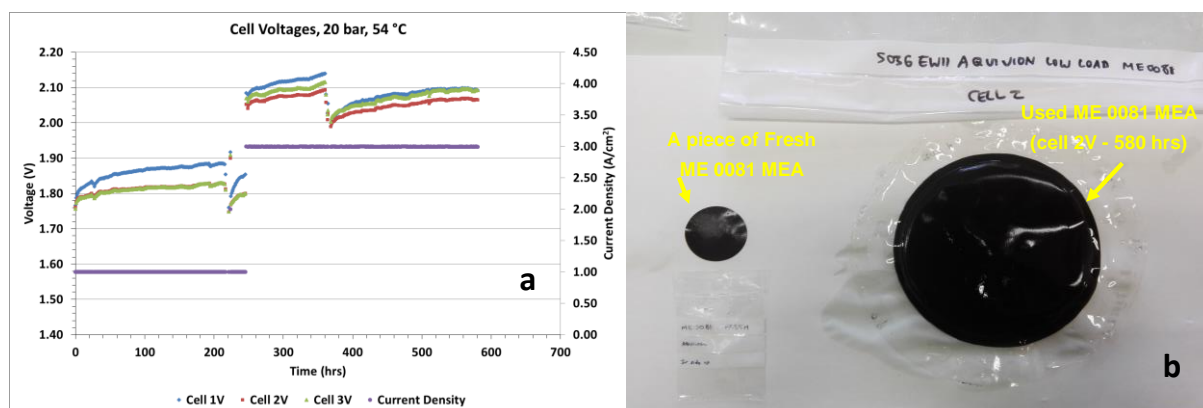


Fig. 5.1 a: Durability test results of a three cell stack with 130 cm² low loaded MEAs (cf. Table 2.3); b: FRESH and USED MEAs MEE0081 picture.

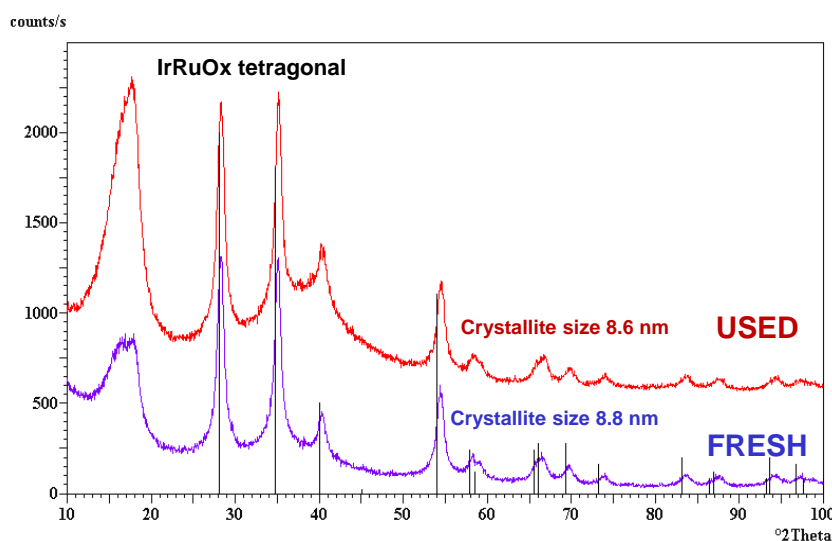


Fig. 5.2 XRD patterns of anode side for FRESH and USED MEAs.

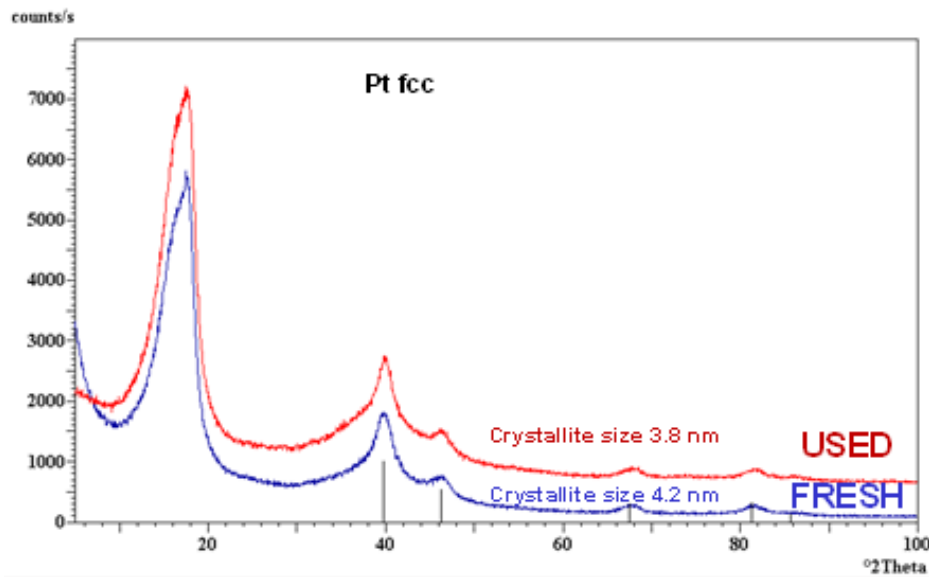


Fig. 5.3
XRD patterns of
cathode side for
FRESH and USED
MEAs.

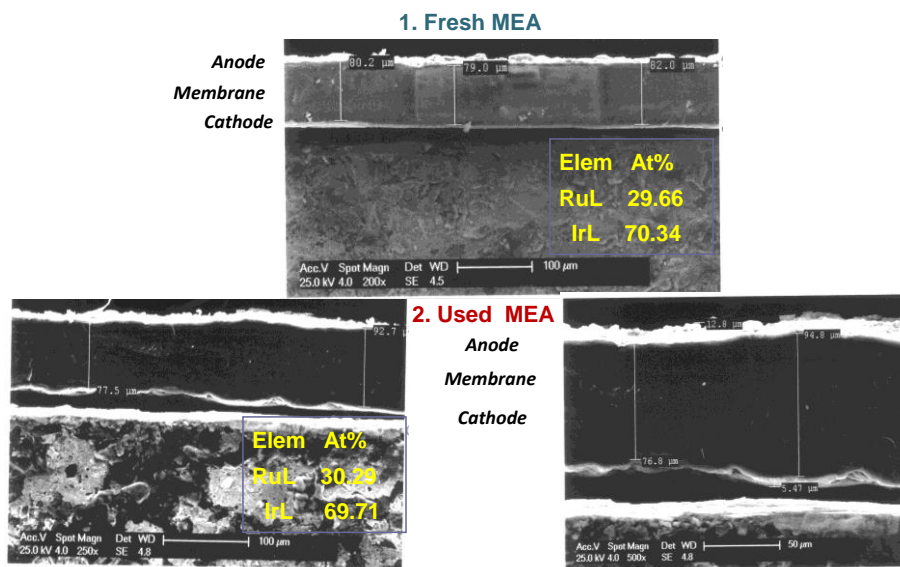


Fig. 5.4
SEM images, in
section view, of
FRESH and USED
MEAs.

Similar analysis was carried out for the cathode side (Fig. 5.3). The MEA is analysed with the cathode side exposed to the X-rays. Also; in this case a slight decrease of crystallite size for the cathode (in the range of the experimental error).

Fig. 5.4 shows the SEM pictures (section view) for the (1) fresh and (2) used MEAs. No change in the catalytic layer or the membrane thickness was recorded after the durability test and there was no evidence of nanoparticles inside the membrane after the test. This suggests no dissolution phenomena were occurring. The EDX analysis of the anode catalytic layer in the MEA before and after the durability test suggests no modification of the Ir/Ru ratio in the bulk. This is observed within the resolution limit of the instrument. No bulk dissolution of ruthenium is evident from the EDX analysis.

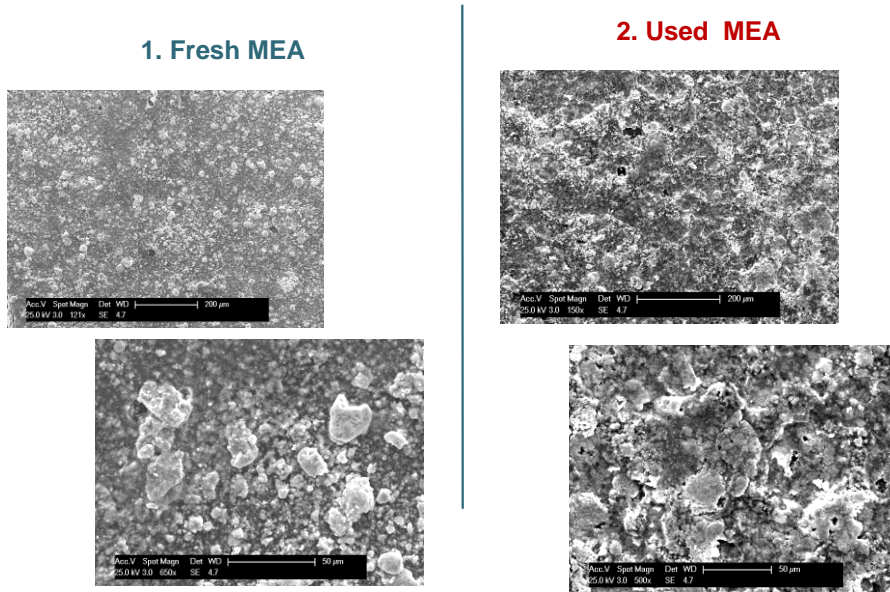


Fig. 5.5
SEM images, in
anode front view, of
FRESH and USED
MEAs.

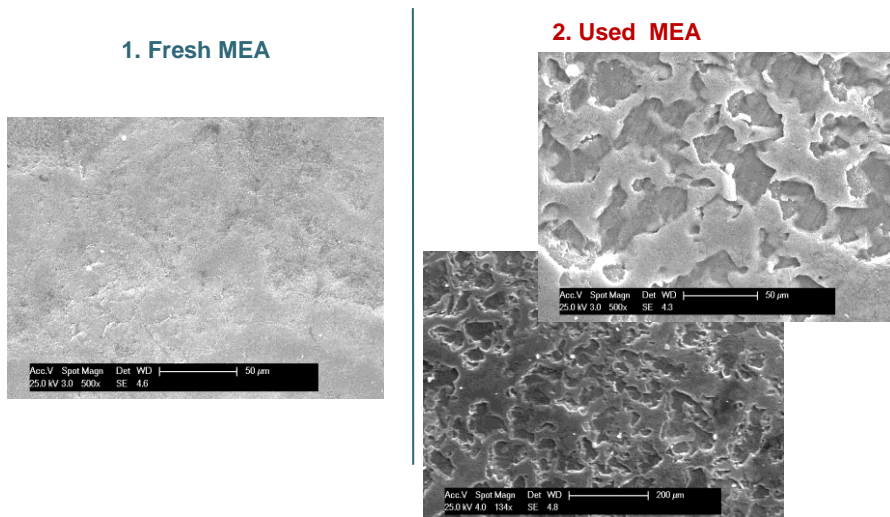


Fig. 5.6
SEM images, in
cathode front view,
of FRESH and USED
MEAs.

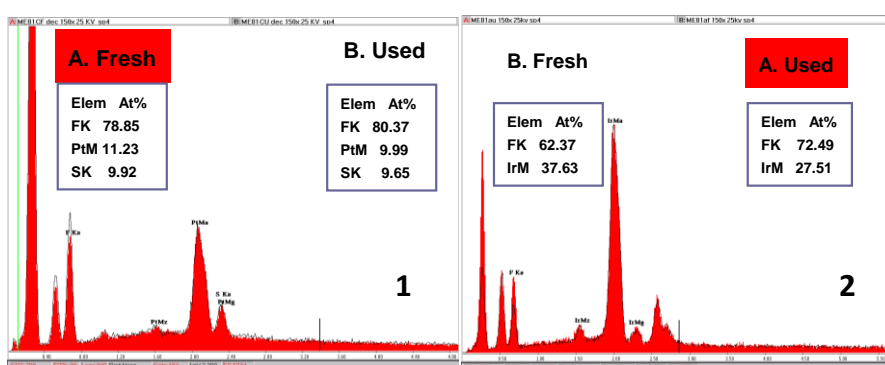


Fig. 5.7
SEM EDX, for the
cathode (1) and
anode (2) side, of
FRESH and USED
MEAs.

Fig. 5.5 shows the SEM pictures (anode front view) for the (1) fresh and (2) used MEAs. No change in the morphology was recorded after the durability test. Fig. 5.6 shows the SEM pictures (cathode front view) for the (1) fresh and (2) used MEAs. An evident delamination/loss of portions of cathode layer in some regions was recorded after the durability test.

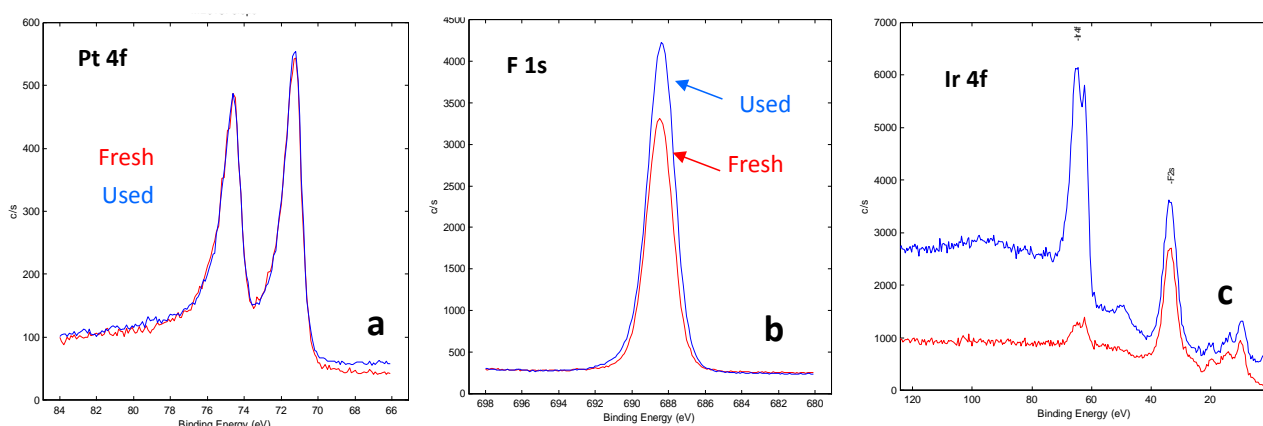


Fig. 5.8 High-resolution XPS spectra for Pt and F signals in the fresh and used cathode side (a, b) and Ir signal in the fresh and used anode side (c).

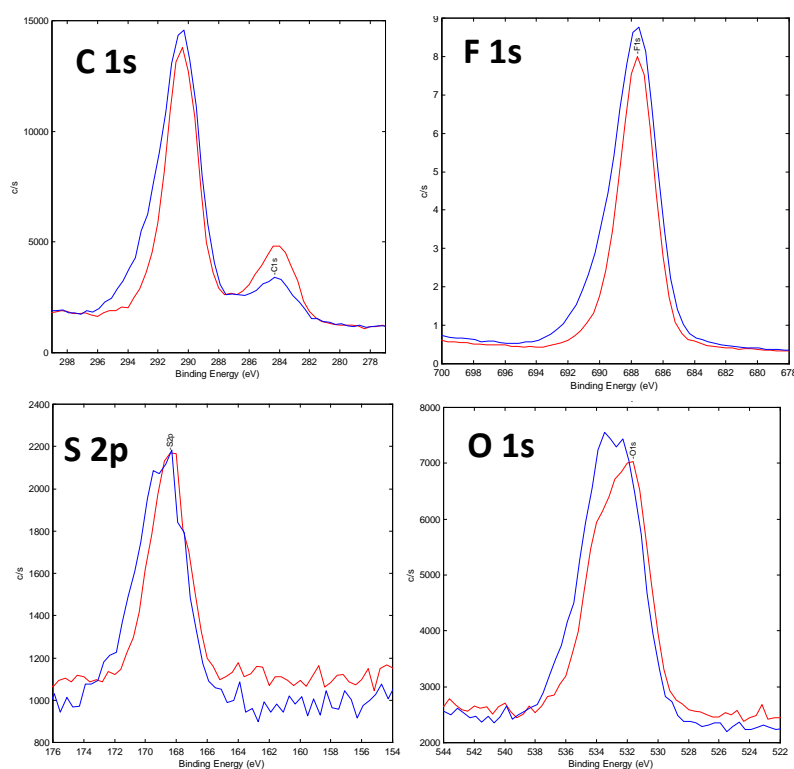


Fig. 5.9 High-resolution XPS spectra for C, F, S and O signals in the fresh and used membrane.

No evident fluorine loss by EDX analysis for the anode and cathode side was observed; on the contrary, a slight increase of F signal in the used cathode, at low magnification 150x, was evident (Fig. 5.7, 1-2). High-resolution XPS spectra for the cathode side (Fig. 5.8, a-b) showed similar Pt signal for Fresh and Used MEAs and a slight increase of F signal in the used MEA. This could be just due restructuring of ionomer around Pt/C. No change in binding energy. For the anode side, in the fresh electrode, the Ir is masked by the ionomer. High-resolution XPS spectra for the membrane (anode and cathode removed) showed similar C, F, S and O signals for Fresh and Used MEAs (Fig. 5.9).

In conclusion, the main evidences of these post operation MEAs characterisations were:

1. No membrane thinning
2. No structure modification for the catalysts
3. No modification of the Ir/Ru atomic ratio
4. Evident delamination/loss of portions of cathode layer (mechanical erosion)